Deep Learning for Glaucoma Detection: R-CNN ResNet-50 and Image Segmentation

Marlene S. Puchaicela-Lozano [1], Luis Zhinin-Vera [2, 3,]*, Ana J. Andrade-Reyes [1], Dayanna M. Baque-Arteaga [1], Carolina Cadena-Morejón [2], Andrés Tirado-Espín [2], Lenin Ramírez-Cando [1], Diego Almeida-Galárraga [1], Jonathan Cruz-Varela [1], and Fernando Villalba Meneses [1]

[1] School of Biological Sciences and Engineering, Yachay Tech University, Urcuquí, Ecuador
[2] School of Mathematical and Computational Sciences, Yachay Tech University, Urcuquí, Ecuador
[3] LoUISE Research Group, I3A, University of Castilla-La Mancha, Albacete, Spain
*Correspondence: luis.zhinin@uclm.es (L.Z.V.)

***Abstract*—Glaucoma is a leading cause of irreversible blindness worldwide, affecting millions of people. Early diagnosis is essential to reduce visual loss, and various techniques are used for glaucoma detection. In this work, a hybrid method for glaucoma fundus image localization using pre-trained Region-based Convolutional Neural Networks (R-CNN) ResNet-50 and cup-to-disk area segmentation is proposed. The ACRIMA and ORIGA databases were used to evaluate the proposed approach. The results showed an average confidence of 0.879 for the ResNet-50 model, indicating it as a reliable alternative for glaucoma detection. Moreover, the cup-to-disc ratio was calculated using Gradient-color-based optic disc segmentation, coinciding with the ResNet-50 results in 80% of cases, having an average confidence score of 0.84. The approach suggested in this study can determine if glaucoma is present or not, with a final accuracy of 95% with specific criteria provided to guide the specialist for an accurate diagnosis. In summary, the proposed model provides a reliable and secure method for diagnosing glaucoma using fundus images.**

***Keywords*—glaucoma, convolutional neural networks, fundus images**

I. Introduction

Glaucoma is an ocular disease characterized by the progressive degeneration of retinal ganglion cells and retinal nerve fiber layers [1]. It has been observed to be associated with elevated Intraocular Pressure (IOP), and causes changes in the optic disc [2]. Moreover, there is a relationship between diabetes mellitus and the influence on biological processes related to glaucoma, suggesting a possible hereditary component. Glaucoma encompasses various subtypes, generally grouped into two main categories: Open-Angle Glaucoma (POAG) and Angle-Closure Glaucoma (PACG); both categories of glaucoma damage the optic nerve, which can later lead to blindness [3]. In addition, since glaucoma is a multifactorial disease [2], several parameters are employed for its detection such as the ratio of the cup and the Cup-to-Disc Ratio (CDR), IOP, Central Cornea Thickness, Neuro Retinal Rim Area, Visual Field, ISNT Rule, and RNFL Thickness [4]. In the case of CDR, the horizontal C/D ratio is usually more significant than the vertical C/D ratio. The disc area is often greater than the cup area; therefore, any change in the optic disc can be glaucoma [5]. Otherwise, Glaucoma could be detected using several techniques such as Optical Coherence Tomography (OCT), Scanning Laser Ophthalmoscopy (SLO), Gonioscopy, and Pachymetry [6–9] (see Table I).

TABLE I. Types of Tests for Glaucoma Diagnosis

Test name	Examine	Reference
Tonometry	Measure the pressure inside the eyes (PIO). Tonometry is implemented by incorporating a vibration sensor in the 3-mirror gonio lens.	Porporato *et al.* [6]
Gonioscopy	Measures the angle between the iris and the cornea.	Bharathi *et al.* [7]
Ophthalmoscopy	Visualize the inside of the fundus and other structures using an ophthalmoscope.	Choudhari *et al.* [8]
Pachymetry	Measures all areas of your eyesight, including your side and peripheral.	Song *et al.* [9]

Despite technological advancements in developing countries, the high costs for diagnosing Glaucoma mean that medical personnel tend to carry out manual assessments. Consequently, glaucoma is frequently detected at advanced stages, leading to blindness. Even the Ecuadorian Glaucoma Society reports that 90% of cases are not seen in time [10]. Thus, precise interpretation of diagnostic tests by ophthalmologists is essential for the early detection of Glaucoma [11, 12]. Therefore, neural networks have arisen for diagnosing several diseases [13–18], such as glaucoma, becoming an essential tool for ophthalmologists.

Generally, most methods developed to diagnose glaucoma [19, 20] evaluate the accuracy. However, in real-life scenarios, the precision and safety are important parameters to implement a procedure. For this reason, this article proposes a novel hybrid method for the early detection of glaucoma using pre-trained ResNet-50 residual convolutional networks and an image

Manuscript received April 25, 2023; revised June 25, 2023; accepted July 11, 2023; published November 10, 2023.

segmentation algorithm to the confidence score using fundus images from ACRIMA and ORIGA databases.

Computer vision techniques, such as machine learning and image processing, have shown promising results in automating the detection of glaucoma from fundus images. Some methods, such as software, can help detect glaucoma by using the Higuchi Fractal Dimension to show that a significant difference in the fractal dimension in patients with glaucoma is greater than in those without glaucoma [21]. Also, neural networks are used to detect pathologies such as glaucoma. This paper develops a method for early detection using pre-trained residual convolutional networks ResNet-50 and a medical image segmentation algorithm from digital fundus images of the eye retina.

The challenges associated with glaucoma detection, such as image quality, dataset imbalance, and diagnostic accuracy, are thoroughly discussed. Additionally, a comprehensive review of state-of-the-art methods, particularly deep learning-based approaches, is presented, highlighting their respective outcomes and advancements. The paper concludes with an examination of future research directions and the potential impact of computer vision techniques in revolutionizing glaucoma diagnosis and management (see Fig. 1).

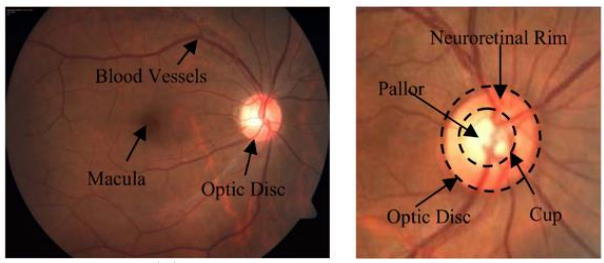

Figure 1. Fundus images showing landmarks named optic disc, optic cup, blood vessels and neuro-retina [11].

II. State of the Art

Today, artificial intelligence in medicine uses machine learning models for tasks like searching for medical data and discovering insights that help boost health outcomes and patient experiences. Due to recent advances in computer science and informatics, Artificial Intelligence (AI) is quickly becoming a solid part of modern healthcare. AI algorithms are used to assist medical professionals in clinical settings and in ongoing research.

For example, researchers are working on the development of different systems such as: development of machine learning models for the diagnosis of bronchitis and pneumonia in resource-limited settings [22], classification of epileptic seizures in real time using Field Programmable Gate Array [23], machine learning algorithms for the prediction of defibrillator performance within clinical engineering [24], and the development of a diagnostic-tool system to identify asthma and chronic obstructive pulmonary disease [25] among other significant advances in the medical field.

Glaucoma exploration methods have been studied to detect glaucoma more accurately. The empirical wavelet transform is based on the Two-Dimensional Fourier-Bessel Series Expansion (2D-FBSE-EWT), which uses the Fourier Bessel Series Expansion (FBSE) spectrum of order zero and order one to limit the detection of glaucoma. The 2D-FBSE-EWT method is also studied on a multi-frequency scale during boundary detection in the FBSE spectrum. The 2D-FBSE-EWT analysis based on multi-frequency scales uses three: total, half, and quarter-frequency scales. These methods are used for the decomposition of fundus images into sub-images. For glaucoma detection from sub images, two methods are used: (1) proposed Method 1, which is a traditional Machine Learning (ML) based method, and (2) proposed Method 2, which is an ensemble ResNet-50 based method. The set is completed by maximums, minimums, averages, and merging. The suggested Method 1 has supplied the best result with order one 2D-FBSE-EWT at full scale. The presented Method 2, containing a full-scale 2D-FBSE-EWT with the fusion ensemble method, provides more accuracy than other ensemble methods [26]. However, a hybrid method is proposed that combines neural networks and computer vision. Convolution neural networks feature 2 VGG architectures, the Inception method, AlexNet, GoogLeNet, and ResNet architectures providing precision levels of up to 100 percent. The various Convolutional Neural Networks (CNN) structures learned from ImageNet (VGG19, VGG16, Inception V2, and ResNet-50) were examined and used as a glaucoma condition classifier in the convolutional neural network.

In the convolutional neural network, the various CNNs and structures learned from ImageNet were analyzed and used as a glaucoma classifier with an average sensitivity of 0.9346 and an average specificity of 0.8580, so that the identification of glaucoma with the elements was obtained with more remarkable precision morphological when applying algorithms operated by CNN [27].

One standard method to improve glaucoma detection accuracy is the optic cup-disc ratio, called CDR. The cup CDR performance is evaluated in two databases: RIMONE v3 and DRISHTI-GS. Although a CDR threshold of 0.5 is primarily used to detect glaucoma, the authors show that a threshold of 0.6 works best. Furthermore, they mention that the CDR method, due to its use of threshold values, is not suitable for detecting glaucoma in the early stage. The CDR method is better for detecting advanced glaucoma, as the method will only identify a fundus image as glaucomatous if the CDR value is 0.6 or greater. This research provides an algorithm with a highly accurate classifier and better performance in detecting early to moderate glaucoma [28]. Therefore, the CDR will also be included in this investigation.

Different computer-assisted methods involve deep convolutional neural networks to detect glaucoma in fundus images. In this study, the researchers propose an advanced form of automatic and accurate recognition of glaucoma. First, a graph-based bulge region detection is used to trim the optic disc and remove redundant parts of the fundus images. Four methods are then used to assemble

convolutional neural network models comprising up to three deep-learning architectures for glaucoma classification. The results show that this model outperforms similar outcomes in the literature [29].

Artificial intelligence coupled with optical coherence tomography creates an algorithm that can effectively create a complex data model for glaucoma detection and diagnosis. In addition, artificial intelligence systems, including machine learning and deep learning techniques, can be used effectively for image reprocessing [30], facilitating the correct diagnosis of glaucoma. So, integrating AI into the healthcare system can be complicated, but it can transform the future management of glaucoma [30].

TABLE II. OVERVIEW OF RELATED WORKS

Approach	Datasets	Results	Reference
A two-dimensional Fourier-Bessel Series Expansion based on empirical wavelet transforms (2D-FBSE-EWT).	RIM-ONE r1 RIM-ONE r2 RIM-ONE r3 Drishti-GS ORIGA	Method 1: From sub-images obtained by order zero and order one 2D-FBSE-EWT. Method 2: Features are extracted from two layers: Last average pool layer, and last new fully connected layer.	Chaudhary and Pachori [26]
A convolution neural network, featuring 2 VGG architectures, the Inception Method, the AlexNet, GoogLeNet, and ResNet architectures.	ImageNet	The identification of glaucoma with the aspects morphological data was obtained with greater precision.	Sunanthini *et al.* [27]
Optic cup-disc ratio (CDR)	RIM-ONE v3 DRISHTI-GS	Datasets marked glaucoma have higher CDR values. However, glaucoma labelled datasets in the RIM-ONE v3 have very low CDR values.	Joshua *et al.* [28]
A glaucoma detection model that uses graph-based saliency and convolutional neural network ensembles.	Images collected from Kim's Eye Hospital patients.	The model outperforms a similar work, as good as, or better than the literature that uses the same dataset.	Serte and Serener [29]
Artificial Intelligence with Machine Learning for softwares in medical devices.	Visual field analysis ORIGA.	SaMD focus on proper clarity level of resultant outcome and algorithm.	Prabhakar *et al.* [30]
An optic disc segmentation model based on the RetinaNet extension with DenseNet.	RetinaNet DenseNet	Efficacy of the deep object detection network is promising to provide segmentation to detect patients in early stages.	AlGhamdi *et al.* [31]
Detection of glaucoma in early stages using features extraction based on deep learning.	Edo Eye Hospital, Pakistan via a Zeiss FF 450 plus fundus camera.	The accuracy is 98.8% on cross-validation and 99% accuracy on the testing dataset.	Mahum *et al.* [32]

Among the methods reviewed in the literature, convolutional neural networks and segmentation algorithms are introduced in this research. The Optic Disc (OD) is essential in fundus imaging to diagnose various diseases, including glaucoma and Diabetic Retinopathy (DR). However, locating and segmenting the DO are challenging tasks. Previous methods have employed a deep Convolutional Neural Network (CNN) without needing handmade functions. An optic disc segmentation model is proposed from fundus images based on the RetinaNet extension with DenseNet that addresses the gradient leakage problem, improves feature propagation, performs deep monitoring, strengthens feature reuse, and reduces the number of parameters. Results show the entire efficacy of the deep object detection network and dense connectivity when applied to fundus imaging, which is a promising step in providing segmentation to detect patients in the early stages of the disease [31]. It seeks to detect glaucoma in its early stages with the help of feature extraction based on deep learning. First, retinal fundus images are used for training and testing the proposed model. In the first step, the images are preprocessed before extracting the region of interest through segmentation. Then, the optic disc features are extracted from the images containing the optic cup using the hybrid feature descriptors, i.e., convolutional neural network, local binary patterns, oriented gradient histogram, and accelerated robust features. In addition, low-level features are extracted with the oriented gradient histogram, while texture features are extracted with the local binary pattern descriptors and accelerated robust features [32].

Furthermore, the high-level features are computed using the convolutional neural network. In addition, a feature selection and classification technique are used to select the most representative features. In the end, multi-class classifiers, i.e., support vector machine, random forest, and K-nearest neighbor, are used to classify fundus images as healthy or diseased. This method achieves 98.8% accuracy in cross-validation and 99% accuracy on the test data set so that it can be used to detect various diseases [32]. A method is proposed to locate the optic nerve head and segment the optic cup/disc in retinal fundus images. The approach is based on a simple two-stage Mask-RCNN comparison method. In the first stage, researchers detect and clip around the optic nerve head and then feed the clipped image as input to the second stage. The second stage network is trained using a weighted loss to produce the final segmentation. To further improve first-stage detection, they propose a new fine-tuning strategy by combining the first stage clipping result with the original training image to train a new detection network using different scales for the proposed network anchors region [33].

A mean absolute error of 0.0430 was achieved in the vertical cup-to-disk ratio in the REFUGE test set compared to 0.0414 obtained using multiple complex ensemble network methods. In detection accuracy, this proposed finetuning strategy improved the detection rate from

96.7% to 98.04% in MESSIDOR and from 93.6% to 100% in the Magrabi datasets [33]. AlexNet, GoogLeNet, and ResNet architectures that provide accuracy levels up to 100 percent. In the convolution neural network, the various CNN structures learned from ImageNet (VGG16, VGG19, Inception V2, and ResNet-50) were analyzed and used as a glaucoma disease classifier. In the convolution neural network, the various CNN, structures learned from ImageNet were analyzed and used as a glaucoma classifier with an average specificity of 0.8580 and an average sensitivity of 0.9346, so the identification, of glaucoma with the aspects Morphological data was obtained with greater precision when applying algorithms operated by CNN [27].

Table II shows a compilation of related works about segmentation algorithm and convolutional neural networks used for the detection of the glaucoma. Most of the methods mentioned solely concentrate on a single verification step, either by utilizing exclusively neural networks or employing a mere detection algorithm. Such an approach may result in a decrease in both the accuracy and confidence levels associated with glaucoma diagnosis, an elevation in the occurrence of false positives or false negatives, and the omission of crucial indicators in glaucoma detection. Consequently, the approach outlined in this study, which combines the Fast ResNet-50 neural network with image segmentation techniques to augment the precision and reliability of glaucoma diagnosis, represents a viable alternative for mitigating these limitations through the incorporation of multiple verification processes.

III. Materials and Methods

In this section the materials and methodology used in the study are presented to develop an algorithm for detecting glaucoma from fundus images. Materials consisted of publicly available databases of fundus images and the methodology involved training and evaluating a Convolutional Neural Network (CNN) using these fundus image datasets.

A. Public Glaucoma Datasets

There are few publicly available databases with glaucoma-labelled images that can be used to evaluate glaucoma classification methods. To this day, in Ecuador, despite the significant concern that Glaucoma represents in the field of ophthalmology, there is no available database to conduct a comprehensive study of this pathology.

Therefore, the authors are pleased to introduce a new publicly available glaucoma-labelled database called: ACRIMA2. All the images of this database come from the ACRIMA project (TIN2013-46751-R), founded by the Ministerio de Economia y Competitividad of Spain, which seeks to develop automated algorithms for retinal disease examination.

The ACRIMA database comprises a total of 705 fundus images, of which 396 are glaucomatous and 309 are nonglaucoma images. These images were acquired from patients with their informed consent, adhering to the ethical standards set forth in the 1964 Declaration of Helsinki. The images were captured using the Topcon TRC retinal camera and ImageNet Capture System, with a field of view of 35°. All patients were selected by experts based on their criteria and clinical findings during the examination. The majority of the fundus images in the database were taken from both the left and right eyes after dilation, with a focus on the optic disc. However, some images were excluded due to the presence of artifacts, noise, or insufficient contrast.

The labeling of all images in the ACRIMA database was performed by two glaucoma specialists with a combined experience of eight years, who provided annotations based solely on the images without considering any other clinical information. However, this initial version of the database can only be utilized for classification purposes, as it does not include optic disc or optic cup segmentation. Fig. 2 provides examples of images contained in the ACRIMA database.

Figure 2. Images of the new public open database. No Glaucoma and Glaucoma fundus images from the new publicly available database (ACRIMA).

In addition to the ACRIMA database, another publicly available database used in this study was the ORIGA database [34], which comprises 382 images of glaucoma and 168 normal images. Table III presents additional databases relevant to glaucoma.

TABLE III. List of All the Publicly Known Databases with Glaucoma Labels

Database	No Glaucoma	Glaucoma	Total	Reference
ACRIMA	309	396	705	GitHub [35]
Drishti-GS1	31	70	101	Sivaswamy *et al.* [36]
sjchoi86-HRF	300	101	401	GitHub [37]
HRF	18	27	45	Budai *et al.* [38]
RIM-ONE	261	194	455	Fumero *et al.* [39]
ORIGA	168	382	650	Zhang *et al.* [34]

B. System Requirements

To conduct all experiments, the Torch-based open-source machine learning framework and NVIDIA Tesla T4

GPU were utilized. PyTorch, which is based on the Torch library and the Python programming language, is an opensource machine learning platform and is considered one of the leading platforms for deep learning research.

C. Preprocessing

The preprocessing phase is a crucial step in many research studies involving data analysis. It involves transforming raw data into a format that is suitable for analysis and machine learning models. In order to classify and locate the optic disc on fundus images, both glaucoma and non-glaucoma eyes were labeled using a bounding box with a radius of 1.5 times the optic disc radius. This cropping technique is based on clinical reasoning that glaucoma typically affects the optic disc and its surrounding area. Furthermore, research conducted by Orlando *et al.* [40] has demonstrated that this method of cropping images around the optic disc is more effective than using the full image. By doing so, the model can learn to accurately locate the glaucoma in the full image and improve the overall accuracy of the classification task. It is important to note that this preprocessing step plays a critical role in ensuring the accuracy and effectiveness of the machine learning model.

D. Pre-trained Region-Based Convolutional Neural Networks (R-CNN) ResNet-50 and Segmentation of Cup-to-Disc Area

The Faster Region-based Convolutional Neural Networks (R-CNN) model is a deep learning network that uses standard Red, Green, and Blue (RGB) inputs to detect objects [41]. In order to ensure the effectiveness of the model, it is important to consider factors such as overfitting and underfitting when working with neural networks [42]. Underfitting occurs when the dataset size is too small, while overfitting occurs when an image is uploaded to the model that does not have the same parameters as those used during training. To address these issues, transfer learning is often used, which involves two stages: a pre-training phase and a phase during which the learned knowledge is applied to a specific task [43].

E. Pre-Trained R-CNN ResNet-50 Architecture

In this study, Pre-Trained R-CNN ResNet-50 models were fine-tuned for the glaucoma assessment task using the Detecto Pytorch version.

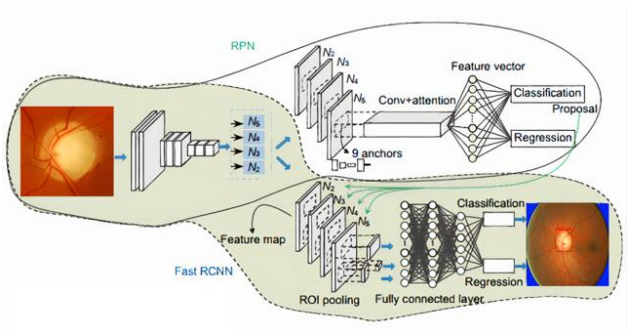

Figure 3. Faster R-CNN is composed of 3 parts: Convolution layers, Region Proposal Network (RPN), and Classes and Bounding Boxes prediction.

The Faster R-CNN model consists of three main components: (1) Convolution layers, where filters are trained to extract the relevant features of the image, specifically those related to glaucoma, (2) Region Proposal Network (RPN), which is a small neural network that slides on the last feature map of the convolution layers to predict all possible locations of glaucoma, including the raw detection with bounding boxes, and (3) Classes and Bounding Boxes prediction, which predict the glaucoma or not glaucoma class based on the degree of confidentiality or confidence threshold of 0.6, along with the corresponding bounding boxes (as shown in adapted Fig. 3). By utilizing these techniques, an effective machine learning model was developed for the detection of glaucoma on fundus images to achieve optimal performance; several adjustments were made before training the model. One such adjustment involved resizing the images to 800 pixels and applying a saturation of 0.3. Additionally, the number of epochs was varied in multiple experiments while keeping other hyperparameters such as batch size and learning rate fixed. In the first experiment, the number of epochs was set to 50, resulting in an overfitting model. In the second experiment, the number of epochs was set to 5, the learning rate was set to 0.001, and a batch size of 1 was used. A random database was used, and a model with a good fit was obtained. These hyper-parameters were selected to achieve the best performance in the experiments.

Furthermore, the performance of the Pre-Trained R-CNN ResNet-50 was evaluated using the final step of Gradient based optic disc segmentation color. This approach involves segmenting the optic disc using color gradients and is known to produce good results. This evaluation allowed for a comparison of the performance of the model with the state-of-the-art techniques for optic disc segmentation.

F. Gradient-Based Optic Disc Segmentation Color

The proposed model used in this study predicts the presence of glaucoma in the fundus images. After the prediction, the model proceeds with the segmentation of the optic disc and optic cup, which is crucial for obtaining better precision in the diagnosis.

To extract blood vessels, the methodology proposed by Abbas *et al.* [44] was utilized. However, since the blood vessels occupy a significant area in the original image, they can become an obstacle in the segmentation phase [45]. Thus, a method was implemented as the first step to eliminate the blood vessels.

After obtaining the image without blood vessels, the next step is to segment the optic disc. To accomplish this, the image must first be converted to grayscale, and an initial location of the optic disc, called ROI or region of interest, must be identified. The K-means method was used for disc segmentation by storing similar measures such as shape and color to distinguish the optic cup area from the optic disc area.

This method allows the Cup-to-Disc Ratio (CDR) to be calculated, which is an important indicator for the diagnosis of glaucoma. According to previous studies [46], CDR values greater than 0.5 indicate patients with

glaucoma, whereas values less than 0.5 indicate normal patients. In this way, the model can provide more accurate results by considering the CDR value in addition to the prediction of the presence of glaucoma.

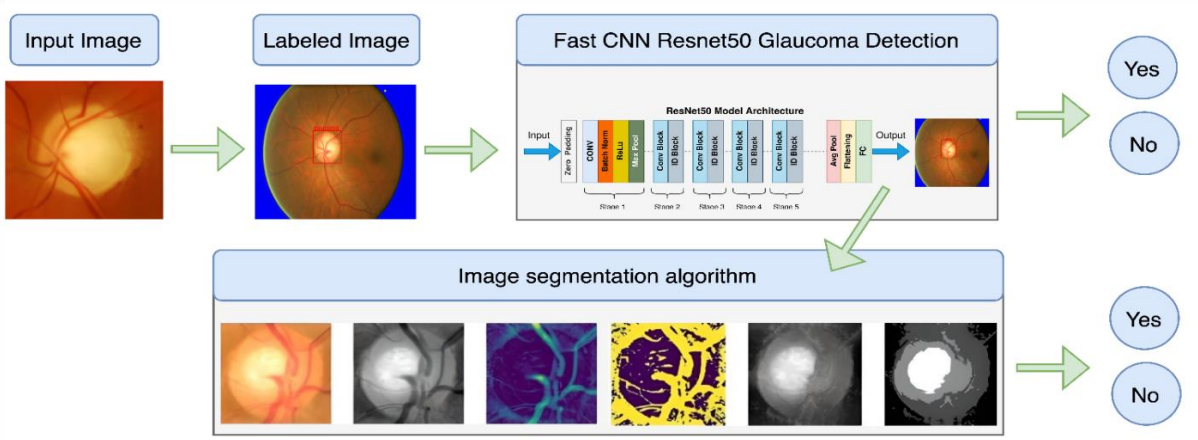

Figure 4. The proposed methodology for glaucoma detection.

Fig. 4 illustrates the segmentation process of the optic disc and optic cup using the K-means method. In the first phase, the Faster R-CNN ResNet-50 model is employed to label the input image and extract relevant features from the fundus image, identifying potential glaucoma sites. By setting a confidence threshold of 0.6, the model provides an accurate prediction of glaucoma presence in the patient. In the second phase, the algorithm performs gradient-based optic disc segmentation to precisely locate the optic disc and optic cup. Calculating the Cup-to-Disc Ratio (CDR) value enables the detection of glaucoma. A CDR value greater than 0.5 indicates the likelihood of glaucoma. By combining the results of both phases, this methodology offers a dual detection approach that ensures an appropriate diagnosis with minimal false positives. Overall, the proposed methodology presents a reliable and accurate approach for early glaucoma detection, facilitating timely diagnosis and treatment to prevent vision loss.

IV. Result

The presented experiment is conducted using fundus images and involves the use of a ResNet-50 Convolutional Neural Network (CNN) and an image segmentation algorithm. The experiment was divided into two stages and was performed on Google Co-lab. In the first stage, ResNet-50 CNN is employed for the detection of glaucoma using a dataset of fundus photographs comprising 1,255 images, with 778 images containing glaucoma and 477 images without glaucoma. The dataset is divided into training (700), validation (400), and testing (155) sets. The training and validation sets contain glaucoma and nonglaucoma labels, respectively (Fig. 5). A learning rate of 0.001, a batch size with a value of 1, and different epoch values (5, 20, and 120) to conduct the experiment are used.

The ResNet-50 model used for glaucoma detection underwent transfer learning techniques during training, indicating that it did not require an extensive number of epochs to learn. After analyzing the validation loss as a function of the number of epochs, it was found that the optimal value of epochs was 5. The graph of the validation loss for 20 epochs indicated overfitting as the curve decreased but did not converge, while the model converged and reached a point of stability with a minimum gap between the final loss values at 5 epochs (Fig. 6).

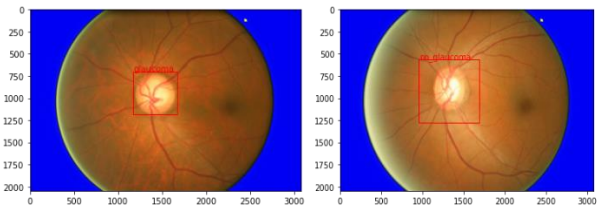

Figure 5. Fundus images with their respective label (glaucoma or no glaucoma).

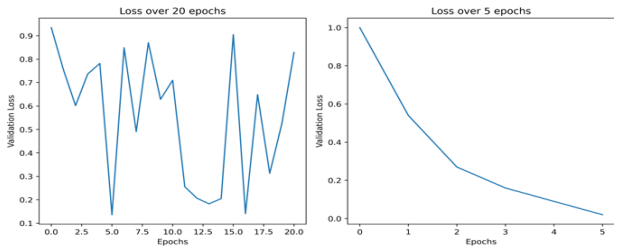

Figure 6. Relationship between Validation Loss and number of Epochs (20 epochs and 5 epochs respectively). For 20 epochs, there was an overfitting; while for 5 epochs, there was an appropriate fitting.

In contrast, Fig. 7 illustrates the glaucoma detection process performed by the model, which employs bounding boxes and a confidence threshold of 0.6 to determine whether the disease is present or not. Only detections with a probability higher than 60% are considered valid.

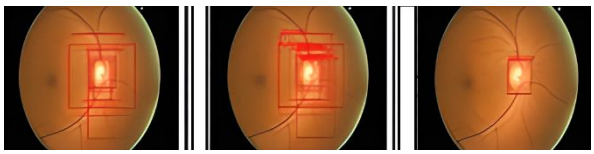

Figure 7. Glaucoma detection by the ResNet-50 convolutional neural network using bounding boxes (confidence threshold = 0.6).

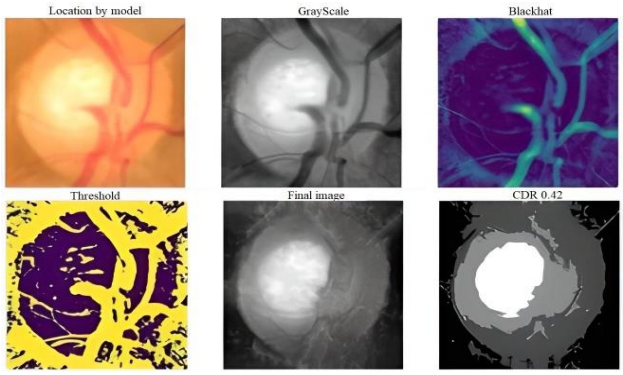

Figure 8. Image segmentation algorithm to detect cup-to-disc-ratio using fundus images. a) ROI localized by the model. b) Convert the original image to grayscale. c) Perform the blackHat filtering on the grayscale image to find the contours. d) Intensify the contours in preparation for the inpainting. e) In-paint the original image depending on the mask and removal of blood vessels. f) Location of the optic and disc cup and calculation of CDR value.

The image shows multiple bounding boxes, and after several iterations, the model detected the presence of glaucoma in specific coordinates with a certainty of 87.9%. In the following stage, optic cup-disc segmentation method was employed that relies on color gradients to identify and locate the Optic Disc (OD) and Optic Cup (OC) using fundus images of the retina. The input image for this process was the Region of Interest (ROI), which was selected based on the highest confidence score obtained by ResNet-50 (greater than 0.6), which was previously used to classify glaucomatous and healthy eyes.

The clinical features necessary to diagnose glaucoma, specifically the optic cup-disc ratio, are in this part of the image. Proposed algorithm automatically performed the OD and OC segmentation using image processing techniques. The input images were converted to grayscale to enhance the contrast of the optic disc compared to the original image. To obtain the areas of the cup and disc were identified the contours, and subsequently was calculated the CDR value. Fig. 8 demonstrates the results of applying the retinal fundus image segmentation algorithm, with a focus on the ROI.

The segmentation of the Optic Cup (OC) is a challenging task compared to the Optic Disc (OD) segmentation, primarily due to the presence of blood vessels, border asymmetry, and the low contrast boundary [46, 47]. In order to address these challenges, the proposed algorithm utilizes morphological operations, specifically blackHat, to eliminate the blood vessels within the Region of Interest (ROI) to prevent vessel edges from being mistakenly identified as cup edges, leading to incorrect segmentation.

Afterward, the algorithm applies an image inpainting technique to fill in the blood vessel areas using the neighboring known areas, replacing the pixel value with the average intensity computed in a small neighborhood around the pixels [48]. The cup and disc regions are then segmented using a K-means clustering-based color segmentation technique [49, 50].

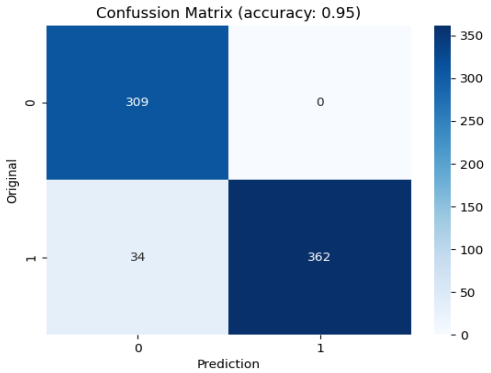

Figure 9. Results of the final fundus image classification of glaucoma (value 1) and non-glaucoma (value 0) cases.

The K-means algorithm is an unsupervised clustering algorithm that groups data points into multiple classes based on their inherent distance from each other [49, 51], and *f* is used to obtain an accurate limit on the cup-disc ratio. In contrast to other techniques, the proposed approach utilizes only the Cup-to-Disc Ratio (CDR) as a parameter for glaucoma detection [52]. The image segmentation algorithm efficiently analyzes instances of suspected glaucoma [53], as CDR is the most widely used physiological parameter for glaucoma detection [49, 50]. Whenever an individual is affected with glaucoma, the CDR relation is altered due to the substantial amount of strain produced in the retina [53]. The threshold taken to differentiate healthy and glaucomatous eyes is 0.5, with values greater than 0.5 considered glaucomatous and values less than 0.5 considered healthy [46]. The area of the OC and OD are calculated using segmentation from the binary images obtained through OD and OC segmentation. The following Eq. (1) calculate the CDR ratio:

$$CDR = 2 \times \left(\frac{cup\ area}{disc\ area} \right) \tag{1}$$

The cup-to-disc area ratio is commonly used for glaucoma detection, where a ratio greater than 0.3 indicates the presence of glaucoma [51]. In this study, an area value of 0.42 and a CDR value of 0.84 were obtained, which exceeds the established threshold. Therefore, it can be determined that the patient is likely to have glaucoma. Overall, the algorithm agreed with ResNet-50 results in 80% of cases, with an average confidence score of 0.84. In the image analyzed, ResNet-50 produced the same diagnosis (patient with glaucoma) with a confidence score of 0.87. By considering both results, it was concluded that the patient is diagnosed with glaucoma. To assist the specialist in giving an appropriate diagnosis, Table IV was constructed. Finally, a final experiment joining both techniques and based on the above table results in 95% accuracy in glaucoma detection using the ACRIMA database. Fig. 9 shows the resulting confusion matrix. To substantiate the metric, Cohen's kappa (κ) was calculated [54]. The value of the kappa coefficient ranges from −1 to 1, where −1 indicates total disagreement, 0 indicates random agreement, and 1 indicates complete

agreement. A kappa value greater than 0.75 is generally considered substantial agreement. The Eq. (2) is as follows:

$$\kappa = \frac{\left(A_C - P_R\right)}{1 - P_R}$$
$$\kappa = \frac{(0.95177305 - 0.5017)}{1 - 0.5017} \quad (2)$$
$$\kappa = 0.903$$

The results are favorable for analysis of this research and show good overall system performance.

TABLE IV. POSSIBLE RESULTS TO GIVE A DIAGNOSIS ABOUT GLAUCOMA, TAKING INTO ACCOUNT THE PREDICTIONS OF RESNET-50 AND CUP-DISC RATIO SEGMENTATION ALGORITHM

ResNet-50 pre-trained with medical images	Image segmentation algorithm	Results
Yes	Yes	Glaucoma
Yes	No	Suspected
No	Yes	Suspected
No	No	Healthy

V. DISCUSSION

In the field of ophthalmology, fundus images are commonly used for the assessment of optic nerve damage and glaucoma detection. This test is widely accessible to the general population and is the primary tool used by specialists for manual evaluation [49, 50]. However, it requires significant expertise and experience to make accurate predictions, and there is still a margin of error due to various factors such as genetics and other pathologies [11, 55]. Additionally, other tests such as Perimetry, Tonometry, Gonioscopy, and OCT are used to study the progression of glaucoma, but they require advanced technology and are typically performed when the disease has already progressed significantly [56, 57]. To address these limitations, researchers have explored automatic evaluation methods for glaucoma detection, such as machine learning algorithms and neural networks that can diagnose the disease with high accuracy [58].

In this study, a new approach is proposed for detecting glaucoma using fundus images. The approach involves using a pre-trained convolutional neural network that was not initially designed for medical images, followed by a feature segmentation algorithm that considers the cup-to-disc diameter ratio relationship. In this study, the initial stage is evaluated by examining the loss function of the ResNet-50 neural network. This parameter helps determine the optimal number of epochs for the model [59]. To do this, tests to determine the number of epochs were conducted that would provide the best fit for the model, using the validation dataset. The results showed that the model achieved good convergence behavior after only five epochs, which means that it could extract general features from the training data and recognize new objects based on these patterns without being limited to memorizing the training data. This is consistent with the concept of transfer learning, which has great potential in automated glaucoma detection using fundus images and convolutional neural networks.

Standard CNN methods require many images, parameters, and computational resources [60]. In contrast, transfer learning involves using a pre-trained convolutional neural network to learn a new task with a small amount of data and high precision [60, 61]. Experimentation demonstrated the effectiveness of this approach, as model worked well with limited data, short training times, minimum generalization error, and lower computational costs.

Furthermore, prior research has established that the ResNet-50 neural network has achieved high accuracy in detecting glaucoma using fundus images. For instance, Ovreiu *et al.* [62] used a ResNet-50 neural network for early-stage glaucoma diagnosis and achieved a precision level of 0.9697. Diaz-Pinto *et al.* [19] utilized various pretrained neural networks, including ResNet-50, in nonmedical imaging, and evaluated them for glaucoma detection, revealing that ResNet-50 achieved an accuracy of 0.9029. Similarly, Chaudhary and Pachori [26] decomposed fundus images into sub-images and employed four pretrained ResNet-50 neural networks, which were trained using the transfer learning method, attaining an accuracy of 0.911. Additionally, Ajitha and Judy [63] proposed a detection system that utilizes a faster region-based CNN (R-CNN) to extract regions of interest from fundus images, with ResNet-50 neural network achieving an accuracy of 0.925 and approximately 0.90 for the DRISHTI and ORIGA datasets, respectively. On the other hand, a study by Joshi *et al*. [64] compared the ResNet-50, VGGNet-16, and GoogLeNet architectures for glaucoma detection, demonstrating that using the PSGIMSR dataset, ResNet-50 attained a higher precision of 0.8860. These authors all agree that ResNet-50 is a suitable alternative for glaucoma diagnosis.

However, according to Ref. [65], high accuracy is not the only objective for good detection, as it is crucial to determine if a CNN model is confident in its result for safe use in real-world applications. Unfortunately, these models often overlook this issue. Therefore, this work focuses on calculating the confidence score, which is an evaluation metric that indicates the probability of the neural network correctly detecting the image [66]. Thus, Fig. 3 illustrates one of the model's predictions. However, the test was conducted with 120 images, and the prediction values ranged between 85% and 97%, with an average value of 86%, even though the prediction threshold is 60%, implying that the ResNet-50 neural network provides dependable results.

The Cup-to-Disc Ratio (CDR) segmentation algorithm aims to detect glaucoma in patients by focusing on the CDR value, which is a marker used for this purpose. Glaucoma is characterized by an increase in intraocular pressure, which affects the internal structures and optic nerve, leading to a phenomenon called cupping. This, in turn, causes an increase in the size of the Optic Cup (OC) relative to the size of the Optic Disc (OD), resulting in an altered CDR value that tends to be higher than normal.

Traditionally, ophthalmologists manually segmented OD and OC in fundus images to calculate CDR, which is a time-consuming and subjective process [47].

Therefore, an automatic and fast segmentation method for OD and OC is required for large-scale and efficient diagnosis of glaucoma. Various methods have been employed for CDR segmentation, including image segmentation algorithms and deep learning techniques. However, some of these methods are time-consuming, require pre- and post-processing, or produce unsatisfactory results. Convolutional Neural Networks (CNNs) have shown excellent results in image segmentation [67]. However, they require a large number of parameters for their model and take a significant amount of time and GPU memory for training, as is the case for CNN and transfer learning approaches for OD segmentation [68]. In the field of computer science for biomedical image analysis, exists Convolutional Neural Networks (CNN) specifically designed for image segmentation tasks, such as the U-Net model [69]. Some researchers have proposed Cup-to-Disc Ratio (CDR) segmentation techniques that are capable of accurately detecting the presence of glaucoma [46–49, 52, 71–73]. For example, Asha *et al.* [74] proposed a segmentation method that achieved a mean error as low as 0.021 (CDR) compared to expert observation. This approach utilizes a color-based segmentation technique that employs K-means clustering to extract the CDR with low computational cost and high accuracy. To achieve a good segmentation of the Optic Disc (OD) and Optic Cup (OC) regions, to remove the blood vessels present in the OD region was proposed, which can interfere with the segmentation process.

TABLE V. COMPARISON OF THE ADVANTAGES AND DISADVANTAGES OF METHODS USED FOR GLAUCOMA DETECTION SIMILAR TO THE APPROACH

Approach	Advantages	Disadvantages	Reference
A novel hybrid approach based on deep learning, feature extraction, feature selection, and ranking technique - MR-MR method and classification – SVM, RF, and KNN.	Robust. It can be used for the detection of several diseases. High accuracy.	Not score of confidence. High number of feature descriptors. Computational complexity.	Mahum *et al.* [32]
An approach using two-dimensional Fourier-Bessel series expansion based empirical wavelet transform and ensemble ResNet-50.	Robust. High accuracy.	High mathematical complexity. Not score of confidence.	Chaudhary and Pachori [26]
Multi-stage for semantic segmentation using the same architecture.	Gives both bounding box and semantic segmentation. High accuracy.	Computational complexity. Not score of confidence	Almubarak *et al.* [33]
A hybrid approach based on faster R-CNN ResNet-50 and the image segmentation algorithm.	Bounding Box Morphological algorithms. Separated stages, high accuracy and confidence score transfer learning low computational complexity. Performs deep diagnosis.	Presence of low percentage of blood vessels in the ROI. Irregular disc shape and optic cup.	Our work

Previous studies have used various image processing techniques, such as histogram thresholding or morphological operations, to improve the segmentation performance slightly [31, 73]. Hybrid approach combines morphological operations, blackHat, and inpainting algorithms to remove the blood vessels while preserving the natural appearance of the preprocessed images [48], as shown in Fig. 8. These results suggest that the presence of blood vessels can affect the segmentation performance, albeit slightly. Furthermore, in the field of image segmentation, the K-means algorithm is widely used for the extraction of regions with varying colors due to its speed and efficiency. This method has been shown to provide results that are in agreement with human observations [49].

Therefore, the proposed approach utilized K-means clustering to achieve better segmentation of the optic cup and disc regions. The K-means algorithm is commonly used for cluster analysis in segmentation and has been applied successfully in various studies. For example, Ayub *et al.* [49] employed K-means clustering for color-based segmentation of optic disc and optic cup regions after applying preprocessing and extracting region of interest. Their method achieved reliable and accurate results, with a 92% accuracy for glaucoma classification. Ali *et al.* [47] developed a novel technique for segmentation of optic disc and optic cup regions, which utilized the fuzzy-based least squares method. This approach effectively extracted features from input images using K-means algorithm to determine the number of fuzzy rules in each fuzzy subsystem. Vimal *et al.* [53] employed the K-means segmentation algorithm using super pixel segmentation, while Arumugam *et al.* [75] segmented the optic disc by applying K-means clustering after preprocessing and removing blood vessels. Thus, the K-means algorithm is more efficient than traditional methods because it limits the size of the search region. In approach, the input consisted of the region of interest, which comprised the optic disc and optic cup area selected by Fast CNN ResNet-50. The diagnosis of glaucoma through fundus images is primarily based on the measurement of Cup-to-Disc Ratio (CDR) [46]. Accurate segmentation of optic disc and cup is crucial for obtaining a reliable CDR measurement, which is essential for clinical assessment [48]. In this context, the proposed algorithm enables the extraction of an image without blood vessels, leading to an optimal segmentation of the cup and disc. The algorithm's predictions are highly accurate in detecting the presence of glaucoma, with the estimated CDR values being very close to the annotations made by clinicians. Moreover, the

algorithm's CDR estimation coincides with the results obtained from Fast CNN, with approximately 80% of estimations being correct and having an average score confidence of 0.84. In future studies, the accuracy of the segmentation algorithm should be evaluated by comparing the CDR value annotated by ophthalmologists with the values obtained through image segmentation. The proposed approach is particularly useful for detecting tiny objects in medical images and for early diagnosis of glaucoma through segmentation of optic disc and cup. In summary, the proposed model presents a reliable approach for the safe diagnosis of glaucoma using fundus images. The combination of Fast CNN for localization and classification of the Optic Nerve Head (ONH) and image segmentation algorithm for CDR calculation provides a useful tool for ophthalmologists in detecting glaucoma. The experimental results show high similarity with annotated values of specialists, with an average score confidence of 0.85. The proposed approach effectively balances the trade-off between performance and computation cost by utilizing Fast CNN pre-trained with medical images and OD/OC segmentation for precise glaucoma detection. Table V summarizes the advantages and disadvantages of the proposed model in comparison to other similar approaches.

VI. Conclusion

This article presents a novel approach to diagnosing glaucoma using fundus images, combining machine learning algorithms and image segmentation techniques. This innovative methodology offers an efficient and accurate alternative to traditional eye fundus examinations performed by ophthalmologists, which are time-consuming and skill-dependent. By leveraging the Fast ResNet-50 neural network for initial glaucoma detection and employing image segmentation for cup-to-disc ratio calculation, the proposed approach demonstrates its effectiveness in accurately diagnosing glaucoma.

Furthermore, the proposed methodology is not only precise and reliable but also user-friendly and accessible to the general public. The proposed envision implementing the model in a mobile application or software, enabling widespread availability and convenience for both ophthalmologists and the general public. This will significantly enhance the accessibility of glaucoma diagnosis and contribute to early detection and treatment to prevent vision loss.

To validate and further improve the accuracy and reliability of the proposed model, future research includes obtaining a comprehensive database, including data from Ecuador. This evaluation will play a crucial role in validating the robustness of this approach. By addressing the limitations of existing work on glaucoma detection, the proposed model has the potential to provide significant support to ophthalmologists and patients worldwide, filling a critical need for improved diagnostic tools in glaucoma management [76–80]. With continuous research and development, the proposed model holds the promise of revolutionizing the field of glaucoma diagnoses and making a substantial impact on the medical community.

Conflict of Interest

The authors declare no conflict of interest.

Author Contributions

L.Z.V. conducted the research, wrote the article, and analyzed the data; (M.P., A.A., D.B.) wrote the article and analyzed the data; (C.C., A.T., L.R, D.A., J.C., F.V.) review the article, proposed different experiments, wrote article; all authors had approved the final version.

References

[1] T. Hasegawa, H. O. Ikeda, S. Iwai, N. Sasaoka, A. Kakizuka, and A. Tsujikawa, "Hop flower extracts mitigate retinal ganglion cell degeneration in a glaucoma mouse model," *Sci. Rep.*, vol. 10, no. 1, pp. 1–9, 2020.

[2] A. Virtanen, J. Haukka, S. Loukovaara, and M. Harju, "Diabetes mellitus and risk of open-angle glaucoma—A population-based follow-up study," *Acta Ophthalmol.*, vol. 101, no. 2, pp. 160–169, Mar. 2023.

[3] J. Jiang *et al.*, "Intraocular asymmetry of visual field defects in primary angle-closure glaucoma, high-tension glaucoma, and normal-tension glaucoma in a Chinese population," *Sci. Rep.*, vol. 11, no. 1, 2021.

[4] B. Turgut, "Pearls for correct assessment of optic disc at glaucoma diagnosis," *US Ophthalmic Rev.*, vol. 10, no. 2, 104, 2017.

[5] M. S. Haleem *et al.*, "A novel adaptive deformable model for automated optic disc and cup segmentation to aid glaucoma diagnosis," *J. Med. Syst.*, vol. 42, no. 1, 2018.

[6] N. Porporato *et al.*, "Understanding diagnostic disagreement in angle closure assessment between anterior segment optical coherence tomography and gonioscopy," *Br. J. Ophthalmol.*, vol. 104, no. 6, pp. 795–799, 2020.

[7] R. B. Bharathi, R. S. Ve, G. Prabhu, and M. S. Swaminathan, "Development of prototype to measure intraocular pressure of eye along with gonioscopy," *IEEE Access*, vol. 10, pp. 7245–7253, 2022.

[8] N. Choudhari, S. Kumar, A. Richhariya, R. Krishnamurthy, R. Priya, and C. Garudadri, "Adaptive optics scanning laser ophthalmoscopy may support early diagnosis of glaucoma," *Indian J. Ophthalmol.*, vol. 70, no. 8, pp. 2877–2882, 2022.

[9] Y. Song, X. Zhang, and R. N. Weinreb, "Gonioscopy-assisted transluminal trabeculotomy in primary congenital glaucoma," *Am. J. Ophthalmol. Case Reports*, vol. 25, 101366, 2022.

[10] A. M. Vásquez. (2018). 90% of glaucoma cases are not diagnosed. [Online]. Available: https://www.edicionmedica.ec/secciones/salud-publica/el-90-de-casos-de-glaucoma-no-son-diagnosticados-91865 (in Spainish)

[11] Y. Wu *et al.*, "Measures of disease activity in glaucoma," *Biosens. Bioelectron.*, vol. 196, Jan. 2022.

[12] J. S. Myers, S. J. Fudemberg, and D. Lee, "Evolution of optic nerve photography for glaucoma screening: A review," *Clin. Exp. Ophthalmol.*, vol. 46, no. 2, pp. 169–176, 2018.

[13] J. Caicho *et al.*, "Diabetic retinopathy: Detection and classification using alexnet, GoogleNet and ResNet-50 convolutional neural networks," *Communications in* Computer *and Information Science*, vol. 1532, pp. 259–271, 2022.

[14] D. N. Niles *et al.*, "COVID-19 pulmonary lesion classification using CNN software in chest X-ray with quadrant scoring severity parameters," *Communications in Computer and Information Science*, vol. 1532, pp. 370–382, 2022.

[15] E. A. Salazar, F. V. Meneses, A. T. Espín, D. A. Marmol, and D. A. Galárraga, "Rapid detection of cardiac pathologies by neural networks using ecg signals (1D) and sECG images (3D)," *Computation*, vol. 10, no. 7, 2022.

[16] E. A. Salazar *et al.*, "Intelligent electromyograph for early detection of myopathy and neuropathy using EMG signals and neural network model," *Communications in Computer and Information Science*, vol. 1648, pp. 32–45, 2022.

[17] J. D. S. Pesántez, E. D. A. Salazar, D. A. Galárraga, G. Salum, F. V. Meneses, and M. E. G. Gomezjurado, "NIFtHool: An

informatics program for identification of NifH proteins using deep neural networks," *F1000Research*, vol. 11, 164, 2022.
[18] O. P. Yanchatuña *et al.*, "Skin lesion detection and classification using convolutional neural network for deep feature extraction and support vector machine," *Int. J. Adv. Sci. Eng. Inf. Technol.*, vol. 11, no. 3, pp. 1260–1267, Jun. 2021.
[19] A. D. Pinto, S. Morales, V. Naranjo, T. Köhler, J. M. Mossi, and A. Navea, "CNNs for automatic glaucoma assessment using fundus images: An extensive validation," *Biomed. Eng. Online*, vol. 18, no. 1, pp. 1–19, 2019.
[20] A. Zafar, M. Aamir, N. M. Nawi, S. Ali, M. Husnain, and A. Samad, "A comprehensive convolutional neural network survey to detect glaucoma disease," *Mob. Inf. Syst.*, vol. 202, 2022.
[21] Q. C. Ngo, S. Bhowmik, M. Sarossy, and D. K. Kumar, "Pupillary complexity for the screening of glaucoma," *IEEE Access*, vol. 9, pp. 144871–144879, 2021.
[22] K. Stokes *et al.*, "A machine learning model for supporting symptom-based referral and diagnosis of bronchitis and pneumonia in limited resource settings," *Biocybern. Biomed. Eng.*, vol. 41, no. 4, pp. 1288–1302, 2021.
[23] R. Sarić, D. Jokić, N. Beganović, L. G. Pokvić, and A. Badnjević, "FPGA-based real-time epileptic seizure classification using artificial neural network," *Biomed. Signal Process. Control*, vol. 62, no. July, pp. 1–10, 2020.
[24] A. Badnjević *et al.*, "Evidence-based clinical engineering: Machine learning algorithms for prediction of defibrillator performance," *Biomed. Signal Process. Control*, vol. 54, 2019.
[25] A. Badnjevic, L. Gurbeta, and E. Custovic, "An expert diagnostic system to automatically identify asthma and chronic obstructive pulmonary disease in clinical settings," *Sci. Rep.*, vol. 8, no. 1, pp. 1–9, 2018.
[26] P. K. Chaudhary and R. B. Pachori, "Automatic diagnosis of glaucoma using two-dimensional fourier-bessel series expansion based empirical wavelet transform," *Biomed. Signal Process. Control*, vol. 64, 102237, 2021.
[27] V. Sunanthini *et al.*, "Comparison of CNN algorithms for feature extraction on fundus images to detect glaucoma," *J. Healthc. Eng.*, vol. 2022, 2022.
[28] A. O. Joshua, G. M. Hocquet, and F. V. Nelwamondo, "Assessment of the cup-to-disc ratio method for glaucoma detection," in *Proc. 2020 International Conference on Saupec Robmech Prasa 2020*, 2020, pp. 1–5.
[29] S. Serte and A. Serener, "Graph-based saliency and ensembles of convolutional neural networks for glaucoma detection," *IET Image Process.*, vol. 15, no. 3, pp. 797–804, 2021.
[30] B. Prabhakar, R. K. Singh, and K. S. Yadav, "Artificial Intelligence (AI) impacting diagnosis of glaucoma and understanding the regulatory aspects of AI-based software as medical device," *Computerized Medical Imaging and Graphics*, vol. 87, 101818, 2021.
[31] M. AlGhamdi, "Optic disc segmentation in fundus images with deep learning object detector," *J. Comput. Sci.*, vol. 16, no. 5, pp. 591–600, 2020.
[32] R. Mahum, S. U. Rehman, O. D. Okon, A. Alabrah, T. Meraj, and H. T. Rauf, "A novel hybrid approach based on deep cnn to detect glaucoma using fundus imaging," *Electron.*, vol. 11, no. 1, 26, 2022.
[33] H. Almubarak, Y. Bazi, and N. Alajlan, "Two-stage mask-RCNN approach for detecting and segmenting the optic nerve head, optic disc, and optic cup in fundus images," *Appl. Sci.*, vol. 10, no. 11, 2020.
[34] Z. Zhang *et al.*, "ORIGA-light: An online retinal fundus image database for glaucoma analysis and research," in *Proc. 2010 Annual International Conference of the IEEE Engineering in Medicine and* Biology *Society, EMBC'10*, 2010, pp. 3065–3068.
[35] GitHub—Cvblab/ACRIMA: ACRIMA project. [Online]. Available: https://github.com/cvblab/ACRIMA
[36] J. Sivaswamy, S. R. Krishnadas, G. D. Joshi, M. J. Ujjwal, and S. Tabish, "Drishti-GS: Retinal image dataset for optic nerve head(ONH) segmentation," in *Proc. 2014 IEEE 11th International Symposium on Biomedical Imaging*, 2014, pp. 53–56.
[37] GitHub—Cvblab/retina_dataset: Retina dataset containing 1) normal 2) cataract 3) glaucoma 4) retina disease. [Online]. Available: https://github.com/cvblab/retina_dataset
[38] A. Budai, R. Bock, A. Maier, J. Hornegger, and G. Michelson, "Robust vessel segmentation in fundus images," *Int. J. Biomed. Imaging*, vol. 201, 2013.
[39] F. Fumero, S. Alayon, J. L. Sanchez, J. Sigut, and M. Gonzalez-Hernandez, "RIM-ONE: An open retinal image database for optic nerve evaluation," in *Proc. IEEE Symp. Comput. Med. Syst.*, no. 478, 2011.
[40] J. I. Orlando, E. Prokofyeva, M. D. Fresno, and M. B. Blaschko, "Convolutional neural network transfer for automated glaucoma identification," in *Proc. 12th Int. Symp. Med. Inf. Process. Anal.*, 2017.
[41] D. Yan *et al.*, "Improved method to detect the tailings ponds from multispectral remote sensing images based on faster r-cnn and transfer learning," *Remote Sens.*, vol. 14, no. 1, 2022.
[42] M. G. Gualsaquí *et al.*, "Convolutional neural network for imagine movement classification for neurorehabilitation of upper extremities using low-frequency EEG signals for spinal cord injury," *Communications in Computer and Information Science*, vol. 1532, pp. 272–287, 2022.
[43] S. Ruder, M. Peters, S. Swayamdipta, and T. Wolf, "Transfer learning in natural language processing tutorial," *Association for Computational Linguistics*, pp. 15–18, 2019.
[44] Q. Abbas, M. E. Celebi, and I. F. García, "Hair removal methods: A comparative study for dermoscopy images," *Biomed. Signal Process. Control*, vol. 6, no. 4, pp. 395–404, 2011.
[45] F. F. Wahid, R. G, S. M. Joseph, D. Swain, O. P. Das, and B. Acharya, "A novel fuzzy-based thresholding approach for blood vessel segmentation from fundus image," *J. Adv. Inf. Technol.*, vol. 14, no. 2, pp. 185–192, 2023.
[46] M. A. F. Granero, A. Sarmiento, D. S. Morillo, S. Jiménez, P. Alemany, and I. Fondón, "Automatic CDR estimation for early glaucoma diagnosis," *Journal of Healthcare Engineering*, 2017.
[47] R. Ali *et al.*, "Optic disk and cup segmentation through fuzzy broad learning system for glaucoma screening," *IEEE Trans. Ind. Informatics*, vol. 17, no. 4, pp. 2476–2487, 2021.
[48] Y. Jiang *et al.*, "Optic disc and cup segmentation with blood vessel removal from fundus images for glaucoma detection," in *Proc. Annual International Conference of the IEEE Engineering in Medicine and Biology Society*, 2018, pp. 862–865.
[49] J. Ayub *et al.*, "Glaucoma detection through optic disc and cup segmentation using k-mean clustering," in *Proc. 2016 International Conference on Computing, Electronic and Electrical Engineering*, 2016, pp. 143–147.
[50] S. B. Sujithra and A. J. Dhas, "Automatic detection of glaucoma based ON cup—Disk ratio with polar segmentation," *Int. J. Eng. Res. Gen. Sci.*, vol. 6, no. 2, pp. 83–90, 2018.
[51] N. Thakur and M. Juneja, "Clustering based approach for segmentation of optic cup and optic disc for detection of glaucoma," *Current Medical Imaging*, vol. 13, no. 1, pp. 99–105, 2017.
[52] H. Fu, J. Cheng, Y. Xu, D. W. K. Wong, J. Liu, and X. Cao, "Joint optic disc and cup segmentation based on multi-label deep network and polar transformation," *IEEE Trans. Med. Imaging*, vol. 37, no. 7, pp. 1597–1605, 2018.
[53] S. Vimal, Y. H. Robinson, M. Kaliappan, K. Vijayalakshmi, and S. Seo, "Retraction note: A method of progression detection for glaucoma using k-means and the GLCM algorithm toward smart medical prediction," *The Journal of Supercomputing*, vol. 79, no. 5. pp. 5841–584, 2021.
[54] A. Ananda, K. H. Ngan, C. Karabağ, A. Ter-Sarkisov, E. Alonso, and C. C. R. Aldasoro, "Classification and visualisation of normal and abnormal radiographs: A comparison between eleven convolutional neural network architectures," *Sensors*, vol. 21, no. 16, 5381, 2021.
[55] M. S. Haleem, L. Han, J. V. Hemert, and B. Li, "Automatic extraction of retinal features from colour retinal images for glaucoma diagnosis: A review," *Comput. Med. Imaging Graph.*, vol. 37, no. 7–8, pp. 581–596, 2013.
[56] S. Subbiah, S. Sankarnarayanan, P. A. Thomas, and C. A. Nelson Jesudasan, "Comparative evaluation of optical coherence tomography in glaucomatous, ocular hypertensive and normal eyes," *Indian J. Ophthalmol.*, vol. 55, no. 4, pp. 283–287, 2007.
[57] P. L. Dabasia. Link to published version: A study of the role of advanced technologies in glaucoma case-finding . [Online]. Available: https://openaccess.city.ac.uk/id/eprint/12364/
[58] J. Camara, A. Neto, I. M. Pires, M. V. Villasana, E. Zdravevski, and A. Cunha, "Literature review on artificial intelligence methods for glaucoma screening, segmentation, and classification," *Journal of Imaging*, vol. 8, no. 2, 2022.

[59] S. Afaq and S. Rao, "Significance of epochs on training a neural network," *Int. J. Sci. Technol. Res.*, vol. 9, no. 06, pp. 485–488, 2020.
[60] S. M. Hassan, A. K. Maji, M. Jasiński, Z. Leonowicz, and E. Jasińska, "Identification of plant-leaf diseases using cnn and transfer-learning approach," *Electron.*, vol. 10, no. 12, 2021.
[61] M. Hussain, J. J. Bird, and D. R. Faria, "A study on CNN transfer learning for image classification," *Adv. Intell. Syst. Comput.*, vol. 840, pp. 191–202, 2019.
[62] S. Ovreiu, I. Cristescu, F. Balta, A. Sultana, and E. Ovreiu, "Early detection of glaucoma using residual networks," in *Proc. 2020 13th International Conference on Communications*, 2020, pp. 161–164.
[63] S. Ajitha and M. V. Judy, "Faster R-CNN classification for the recognition of glaucoma," *Journal of Physics: Conference Series*, vol. 1706, no. 1, 12170, 2020.
[64] S. Joshi, B. Partibane, W. A. Hatamleh, H. Tarazi, C. S. Yadav, and D. Krah, "Glaucoma detection using image processing and supervised learning for classification," *J. Healthc. Eng.*, vol. 202, 2022.
[65] X. He, Y. Chen, and L. Huang, "Toward a trustworthy classifier with deep CNN: Uncertainty estimation meets hyperspectral image," *IEEE Trans. Geosci. Remote Sens.*, vol. 60, pp. 1–15, 2022.
[66] E. Scheme and K. Englehart, "A comparison of classification based confidence metrics for use in the design of myoelectric control systems," in *Proc. Annual International* Conference *of the IEEE Engineering in Medicine and Biology Society*, 2015, pp. 7278–7283.
[67] R. Priyanka, P. S. J. G. Shoba, and D. A. B. Therese, "Segmentation of optic disc in fundus images using convolutional Neural networks for detection of glaucoma," *Int. J. Adv. Eng. Res. Sci.*, vol. 4, no. 5, pp. 170–179, 2017.
[68] K. K. Maninis, J. P. Tuset, P. Arbeláez, and L. V. Gool, "Deep retinal image understanding," *Lecture Notes in Computer Science (Including Subseries Lecture Notes in Artificial Intelligence and Lecture Notes in Bioinformatics)*, pp. 140–148, 2016.
[69] R. Shinde, "Glaucoma detection in retinal fundus images using U-Net and supervised machine learning algorithms," *Intell. Med.*, vol. 5, 100038, Jan. 2021.
[70] V. Mahalakshmi and S. Karthikeyan, "Clustering based optic disc and optic cup segmentation for glaucoma detection," *Int. J. Innov. Res. Comput. Commun. Eng.*, vol. 2, no. 4, pp. 3756–3761, 2014.
[71] A. Mvoulana, R. Kachouri, and M. Akil, "Fully automated method for glaucoma screening using robust optic nerve head detection and unsupervised segmentation based cup-to-disc ratio computation in retinal fundus images," *Comput. Med. Imaging Graph.*, vol. 77, 101643, 2019.
[72] R. G. Ramani and J. J. Shanthamalar, "Improved image processing techniques for optic disc segmentation in retinal fundus images," *Biomed. Signal Process. Control*, vol. 58, 101832, 2020.
[73] S. Pathan, P. Kumar, R. M. Pai, and S. V Bhandary, "Automated segmentation and classifcation of retinal features for glaucoma diagnosis," *Biomed. Signal Process. Control*, vol. 63, 102244, 2021.
[74] A. M. Jose, "A novel method for glaucoma detection using fundus images," in *Proc. 2015 Int. Conf. Circuit, Power Comput. Technol.*, 2015, pp. 10–12.
[75] G. Arumugam, S. Nivedha, and I. Ntroduction, "Optic disc segmentation based on independent component analysis and K-means clustering abstract," *Int. J. Emerg. Trends Technol. Comput. Sci.*, vol. 2, no. 6, pp. 246–251, 2013.
[76] D. A. Galárraga *et al.*, "Glaucoma detection through digital processing from fundus images using MATLAB," in *Proc. 2021 Second International Conference on Information Systems and* Software *Technologies (ICI2ST)*, 2021, pp. 39–45.
[77] P. Carrillo *et al.*, "Comparison between two novel approaches in automatic breast cancer detection and diagnosis and its contribution in Military defense," *Developments and Advances in Defense and Security . Smart Innovation, Systems and Technologies*, vol. 255, 2022.
[78] D. V. U. PA *et al.*, "Analysis and evaluation of the systems used for the assessment of the cervical spine function: A systematic review," *J. Med. Eng. Technol.*, vol. 5, no. 5, pp. 380–393, 2021.
[79] E. D. A. Salazar *et al.*, "Design of a glove controlled by electromyographic signals for the rehabilitation of patients with rheumatoid arthritis," in *Proc. Conference on Information and Communication Technologies of Ecuador*, 2020, vol. 1307, pp. 3–11.
[80] N. Y. G. Castillo *et al.*, "A machine learning approach for blood glucose level prediction using a LSTM networ," in *Proc. International Conference on Smart Technologies, Systems and Applications*, 2022, vol. 1532.